

COMPARISON OF AEROSOL OPTICAL DEPTH INFERRED FROM SURFACE
MEASUREMENTS WITH THAT DETERMINED BY SUN PHOTOMETRY FOR
CLOUD-FREE CONDITIONS AT A CONTINENTAL U.S. SITE

M. H. Bergin, S. E. Schwartz, R. N. Halthore, J. A. Ogren, and D. L. Hlavka

Original Manuscript: August 1998

Published in
Journal of Geophysical Research
[vol. 105, 6807-6816, 2000]

By acceptance of this article, the publisher and/or recipient acknowledges the U.S. Government's right to retain a nonexclusive, royalty-free license in and to any copyright covering this paper.

Research by BNL investigators was performed under the auspices of the U.S. Department of Energy under Contract No. DE-AC02-98CH10886.

Comparison of aerosol optical depth inferred from surface measurements with that determined by Sun photometry for cloud-free conditions at a continental U.S. site

M. H. Bergin,^{1,2,3} S. E. Schwartz,¹ R. N. Halthore,¹ J. A. Ogren,²
D. L. Hlavka⁴

Abstract. Evaluation of the forcing of climate by aerosol scattering of shortwave radiation in cloud-free conditions (direct aerosol forcing) requires knowledge of aerosol optical properties on relevant spatial and temporal scales. It is convenient to measure these properties at the surface. However, before these measurements can be used to quantitatively estimate direct climate forcing, it is necessary to determine the extent to which these properties are representative of the entire atmospheric column. In this paper we compare aerosol optical depth (AOD) determined by Sun photometry at the Southern Great Plains (SGP) Atmospheric Radiation Measurement (ARM) site in north central Oklahoma for several cloud-free days with estimates of AOD based on two methods. First, the aerosol extinction measured at the surface (taken as the sum of the aerosol scattering and absorption coefficients at instrumental relative humidity of ~20%) is multiplied by the mixing height determined from temperature profiles from radiosonde measurements. Even under conditions of vigorous midday mixing this approach underestimates AOD by as much as 70% using dry aerosol measurements and by roughly 40% when hygroscopic growth of aerosol under ambient relative humidity is taken into account. This discrepancy is attributed primarily to underestimation of aerosol column extinction, as confirmed by examination of normalized aerosol backscatter profiles obtained from micropulse lidar (MPL), which show substantial contributions of aerosol loading above the atmospheric boundary layer. The second approach uses MPL profiles of normalized aerosol backscatter to estimate the vertical profile of aerosol extinction using surface values. The resulting AOD's are on average 30% less than measured values. This discrepancy is attributed to hygroscopic growth of aerosols in the atmospheric column. The results show that at the SGP site even under conditions of vigorous mixing in the atmospheric boundary layer the aerosol optical depth cannot be estimated with surface measurements of aerosol extinction unless information on the vertical profile of aerosol extinction is taken into account.

1. Introduction

The decrease in planetary absorption of shortwave radiation due to scattering by anthropogenic aerosols during clear-sky conditions, termed direct aerosol radiative forcing, is estimated to be roughly 1 W m^{-2} on a global annual average [Charlson *et al.*, 1992; Kiehl and Briegleb, 1993; Intergovernmental Panel on Climate Change, 1995] and may be as great as 50 W m^{-2} locally and instantaneously near source regions [Schwartz, 1996]. In large part because of the patchy nature of aerosol forcing on both temporal and spatial scales, as well as the general lack of knowledge of aerosol radiative properties, the uncertainty in estimates of global mean direct aerosol radiative forcing is at least

a factor of two [Penner *et al.*, 1994; IPCC, 1995; Schwartz and Andreae, 1996; Quinn *et al.*, 1996].

The key aerosol property governing direct shortwave radiative forcing is aerosol optical depth (AOD) (integral of the aerosol extinction coefficient with height; throughout the paper the term AOD refers to the vertical optical depth, i.e., air mass equal to one) which is a measure of the aerosol loading, or “extensive” aerosol property [Ogren *et al.*, 1996]. Pertinent “intensive” aerosol properties are single scattering albedo (fraction of aerosol extinction that is due to scattering versus absorption), and upscatter fraction (fraction of light scattered into the upward hemisphere) [Charlson *et al.* 1992; Haywood and Shine, 1995; Boucher and Anderson, 1995; Nemesure *et al.*, 1995; Schwartz 1996]. Estimates of direct radiative forcing have generally relied on surface measurements of aerosol radiative properties [Charlson *et al.*, 1992; IPCC, 1995] under the assumption that aerosol properties over the entire tropospheric column are similar to those at the surface. However, it has yet to be shown on a systematic basis that aerosol optical properties at the surface are suitably representative of the integrated column properties to justify this assumption.

Several recent studies have raised concern over the determination of AOD by Sun photometry [Kato *et al.*, 1997; Halthore *et al.*, 1998]. Model estimates of the broadband direct normal solar irradiance during cloud-free conditions based on AOD values determined from Sun photometry agree with measured values, but the same AOD's lead to an overestimation

¹Environmental Chemistry Division, Brookhaven National Laboratory, Upton, New York.

²Climate Monitoring and Diagnostics Laboratory, National Oceanic and Atmospheric Administration, Boulder, Colorado.

³Now at Georgia Institute of Technology, School of Civil and Environmental Engineering and School of Earth and Atmospheric Sciences, Atlanta, Georgia.

⁴Science Systems and Applications, NASA Goddard Space Flight Center, Greenbelt, Maryland.

of the diffuse downwelling irradiance by as much as 40%. A possible explanation for this discrepancy is an unaccounted for continuum-like atmospheric absorptance over the solar spectrum [Kato *et al.*, 1997; Halthore *et al.*, 1998]. Halthore *et al.* [1998] suggest that AOD inferred by Sun photometry may be overestimated by ~ 0.02 . For this reason it is important to ascertain whether the aerosol optical depth measured by Sun photometry is identical to that given by the column integral of aerosol extinction.

In principle such a closure experiment might be carried out by comparing AOD estimated by Sun photometry with in-situ vertical integrated aerosol extinction measurements from an aircraft. However, such ideal experiments present challenging experimental difficulties [Remer *et al.*, 1997] and are generally quite limited because of the effort and expenses associated with aircraft operations. Although the aerosol scattering coefficient is readily measured by means of an integrating nephelometer, the measured value is generally not equal to the ambient scattering coefficient because the ambient RH is not identical to that in the nephelometer due to heating of the sample airstream within the nephelometer control volume [Bergin *et al.*, 1997]. Clarke *et al.* [1996] estimated the change in aerosol optical depth based on size-resolved aerosol measurements for two aircraft descents during clear-sky conditions over the Atlantic Ocean. They found that in the case of polluted continental air the estimated AOD was within a few percent of AOD measured by Sun photometry, whereas for a case impacted by Sahara dust the AOD was underestimated by $\sim 50\%$. The discrepancy was attributed to horizontal spatial variability in aerosol. Remer *et al.* [1997] compared AOD measurements made at the surface with AOD estimates based on the vertical integration of humidity corrected extinction measurements made for several flights off the east coast of the United States. The estimated AOD's were typically 50% less than measured values. The difference was considered most likely due to aerosols aloft, which were not accounted for because the flights were confined to the lower 2 km of the atmosphere. Hegg *et al.* [1997] measured vertical profiles of aerosol extinction as well as the humidity dependence of aerosol light scattering from an aircraft for several clear-sky days off the east coast of the United States. Aerosol optical depths estimated from the vertical profiles were within $\sim 15\%$ of that estimated by Sun photometry. In the present study we take an alternative approach of estimating AOD from surface-based measurements of aerosol scattering and absorption, which, although subject to the concerns raised above regarding relative humidity (RH) influence, can in principle be much more widespread and continuous than aircraft measurements.

Several previous studies have attempted to integrate aerosol surface measurements with height in order to estimate aerosol properties pertinent to radiative forcing of climate [Quinn *et al.*, 1996]. Hoppel *et al.* [1990] estimated AOD's in the marine boundary layer for several days based on surface measurements of aerosol size distributions and scattering coefficients. The estimated AOD's were highly correlated with surface measurements but were a factor of 2 to 4 lower than the direct measurements. The discrepancy was attributed to the lack of knowledge of the vertical profiles of aerosol extinction. Veeffkind *et al.* [1996] estimated AOD's for three clear-sky days in the Netherlands based on surface measurements of aerosol scattering coefficient and its dependence on RH, together with estimates of mixing height based on lidar measurements, under the assumptions that the aerosol was entirely within the mixed layer

and that the single scattering albedo was close to unity. The estimated and measured AOD's agreed within roughly 20%.

In this paper we report aerosol measurements made at the Southern Great Plains (SGP) Atmospheric Radiation Measurement (ARM) site in Oklahoma, where aerosol optical properties related to climate forcing are continuously being measured at the surface. Aerosol properties measured at the surface include aerosol light scattering coefficient measured at three wavelengths and absorption coefficient. The measurements are made at a low reference relative humidity ($\sim 20\%$) in order to measure the properties that are intrinsic to the aerosol and independent of atmospheric relative humidity. Measurements of aerosol column properties include AOD at six wavelengths by Sun photometry and the vertical profile of normalized aerosol backscattering by a micropulse lidar (MPL).

2. Theory and Approach

The first objective is to ascertain the accuracy to which aerosol optical depth can be estimated based on surface measurements of aerosol extinction and mixing height estimates. The second, related objective is to ascertain the accuracy of estimating AOD using normalized lidar backscatter profiles to scale extinction measurements at the surface with height in order to include the effect of the vertical structure of aerosol extinction. In this section, the theoretical framework for estimating aerosol optical depth using both approaches is presented.

The AOD τ at a given wavelength is equal to the integral of the particle extinction coefficient σ_{ep} , with height from the surface to the top of the atmosphere, toa;

$$\tau = \int_{\text{sfc}}^{\text{toa}} \sigma_{ep}(\text{RH}) dz \quad (1)$$

because surface aerosol measurements are made at a dry reference RH (typically $\sim 20\%$), relating AOD to the measured extinction coefficient requires that equation (1) be written in terms of particle extinction coefficient at a dry reference relative humidity, $\sigma_{ep}(\text{RH}_{\text{ref}})$, as

$$\tau = \int_{\text{sfc}}^{\text{toa}} \sigma_{ep}(\text{RH}_{\text{ref}}) F_{ep}(\text{RH}) dz \quad (2)$$

where $F_{ep}(\text{RH})$ is the light extinction hygroscopic growth factor which is equal to $\sigma_{ep}(\text{RH})/\sigma_{ep}(\text{RH}_{\text{ref}})$. Equation 2 can also be written in terms of the aerosol scattering, $\sigma_{sp}(\text{RH}_{\text{ref}})$, and absorption coefficients, $\sigma_{ap}(\text{RH}_{\text{ref}})$, at a dry reference RH with the hygroscopic growth factors for light scattering and absorption of $F_{sp}(\text{RH})$ and $F_{ap}(\text{RH})$ as

$$\tau = \int_{\text{sfc}}^{\text{toa}} \sigma_{sp}(\text{RH}_{\text{ref}}) F_{sp}(\text{RH}) dz + \int_{\text{sfc}}^{\text{toa}} \sigma_{ap}(\text{RH}_{\text{ref}}) F_{ap}(\text{RH}) dz \quad (3)$$

The first approach to estimating aerosol optical depth is based on the assumption that the aerosol is entirely within a well-mixed boundary layer of height H_{ML} , where H_{ML} is determined as the transition between an unstable to stable atmospheric lapse rate. The aerosol extinction coefficient at the reference RH is determined from measurements of the aerosol scattering and absorption coefficients at the surface. Under these assumptions the aerosol optical depth using approach I, τ_I , can be written as

$$\tau_I = [\sigma_{sp}(sfc) F_{sp}(RH) + \sigma_{ap}(sfc) F_{ap}(RH)] H_{ML} \quad (4)$$

The second approach infers the vertical profile of aerosol extinction from the magnitude of the attenuation-and range-corrected profile of aerosol backscatter return, normalized to the surface value, as determined by micropulse lidar (MPL), scaled by the aerosol extinction coefficient measured at the surface. The aerosol optical depth using approach II, τ_{II} , is estimated as follows:

$$\tau_{II} = [\sigma_{sp}(sfc) F_{sp}(RH) + \sigma_{ap}(sfc) F_{ap}(RH)] \int_{sfc}^{toa} \beta_{\pi}(z) / \beta_{\pi}(sfc) dz \quad (5)$$

where $\beta_{\pi}(z)$ is the attenuation-and range-corrected 180° MPL return signal as a function of height. Implicit in equation (5) is that the ratio of aerosol extinction to backscattering, σ_{ep}/β_{π} , is constant with height. In addition, MPL profiles of aerosol backscatter can be used to estimate the fraction of aerosol backscatter due to aerosol within the boundary layer:

$$F_H = \frac{H_{ML} \int_{sfc}^{H_{ML}} \beta_{\pi}(z) dz}{\int_{sfc}^{toa} \beta_{\pi}(z) dz} \quad (6)$$

In this paper we use surface measurements of aerosol scattering and absorption coefficients made at a low reference relative humidity (~20%) together with mixing heights derived from sonde measurements to estimate AOD's based on equation (4) for several cloud-free days at the SGP ARM site. The comparisons are made at 1730 UTC (~ 1130 LT) since this time period corresponds roughly to the daily maximum in surface shortwave irradiance. The time also coincides with the launching of radiosondes which supply vertical profiles of temperature and RH. We also use normalized attenuation-and range-corrected 180° MPL returns to scale surface measurements of the aerosol extinction with height to estimate aerosol optical depth based on equation (5). The estimated aerosol optical depths are compared with AOD's measured by Sun photometry.

3. Experimental Methods

3.1. Measurement of Aerosol Scattering and Absorption at the Surface

Several aerosol properties are measured continuously at the surface at the SGP ARM site. Ambient air is sampled through a

10m-high stack at 800 l min⁻¹. A portion of the flow (150 l min⁻¹) is heated to maintain an RH of ~40%. A portion of the conditioned airstream (30 l min⁻¹) then passes through an impactor with a 10- μ m particle diameter cut size. The airstream is then sampled by an integrating nephelometer (TSI model 3653) and a Particle Soot Absorption Photometer, PSAP (Radiance Research). The nephelometer heats the air by an additional several degrees (5.0 °C \pm 0.5 °C based on 1-min nephelometer data at the SGP site) resulting in a further decrease in RH. The nephelometer measures the aerosol scattering coefficient, σ_{sp} , at wavelengths of 450, 550, and 700 nm. Noise levels for scattering coefficient measurements for the SGP nephelometer as determined from the standard deviations of mean values for filtered air are 0.33, 0.19, and 0.46 Mm⁻¹ for wavelengths of 450, 550, and 750 nm, respectively. Scattering coefficient measurements are not corrected for nephelometer nonidealities as described by *Anderson and Ogren* [1998] since the particles are predominantly in the submicron mode at the SGP site [*Sheridan et al.*, 1998], where such corrections are typically less than 10%. Scattering coefficient measurements are used to determine the Ångström exponent, \hat{a} (negative slope of the scattering coefficient versus wavelength curve when plotted on a log-log scale), which supplies qualitative information on particle size. The PSAP measures the aerosol absorption coefficient, σ_{ap} , at a wavelength of 565 nm. Both σ_{ap} and σ_{sp} (measured at 550 nm) are used to estimate the single scattering albedo ω_0 (ratio of aerosol scattering to extinction). The aerosol observation system (AOS) is similar to that at aerosol monitoring stations maintained by the National Oceanic and Atmospheric Administration (NOAA) Climate Monitoring and Diagnostics Laboratory (CMDL) [*Ogren et al.*, 1996, *Bergin et al.*, 1997].

3.2. Aerosol Optical Depth

Atmospheric extinction is determined at wavelengths of 414, 499, 608, 662, 859, and 938 nm from measurements of diffuse and total downwelling solar irradiance using a Multifilter Rotating Shadowband Radiometer (MFRSR) [*Harrison et al.*, 1994; *Michalsky et al.*, 1995]. At each wavelength the direct beam signal is evaluated as total minus diffuse signal and the direct normal signal is determined by multiplying the direct beam signal by the secant of the solar zenith angle. Extinction optical depths are then determined by Langley analyses [*Harrison et al.*, 1994; *Michalsky et al.*, 1995]. Apparent aerosol optical depth is obtained by subtracting extinction due to Rayleigh scattering and known gaseous absorption from measured extinction optical depth.

The precision of the AOD estimate is ± 0.02 [*Halothore et al.*, 1997]. As previously mentioned, it has been suggested that the AOD is overestimated by ~0.02, due to the absorption of shortwave radiation by an unaccounted for species [*Halothore et al.*, 1998]. The AOD's reported in this paper are the "apparent" AOD's that may include a contribution of ~0.02 from the unaccounted for absorbing species. The Ångström exponent of the apparent AOD is evaluated as the negative slope of the AOD versus wavelength curve when plotted on a log-log scale which is estimated using 450-and 700-nm wavelengths (i.e., Ångström exponent = $-\log(\tau_{700}/\tau_{450}) / \log(700/450)$).

3.3. Vertical Distribution of Normalized Aerosol Backscatter

A micropulse lidar (MPL) is used to determine the normalized attenuation-and range-corrected 180° backscatter profile with

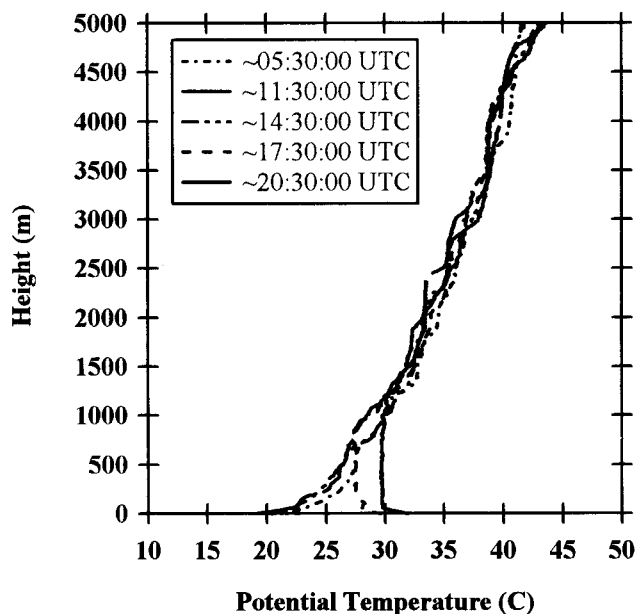


Figure 1. Potential temperature profiles versus height estimated from balloon sonde measurements of temperature for several times during the day of September 4, 1996

height at a wavelength of 523 nm [Spinhirne, 1993]. The vertical sampling resolution is 300 m, with a laser pulse frequency of 2500 Hz. Retrievals of aerosol backscatter with height, $\beta_{\pi}(z)$, are averaged over 1-min time intervals. The MPL is calibrated during a 60-90 min cloud-free period when aerosol loadings are low (i.e., AOD less than 0.1). The retrievals are calibrated by making the assumption that the backscatter at 523 nm for layers in the upper troposphere (~7-13 km) is entirely due to molecular scattering. The attenuation in the signal due to lower tropospheric aerosol is estimated from the MPL signal profile under the assumption of an aerosol extinction to 180° backscatter ratio of 23 [Spinhirne *et al.*, 1980]. The integrated MPL signal in the upper troposphere is then fit to the integrated molecular signal in order to obtain a calibration value. The calibration value represents the adjustment factor applied to the MPL signal for a known scattering cross section (due to Rayleigh scattering). Once the calibration value is obtained it is applied to the backscatter signal to get the backscatter cross section ($\text{m}^{-1} \text{sr}^{-1}$).

3.4. Atmospheric State Parameters

Vertical profiles of temperature, pressure, and relative humidity are regularly measured at the SGP ARM site by means of balloon-borne radiosondes. Here we use potential temperature profiles to estimate mixing heights at 1730 UTC (~1130 local standard time) for cloud-free days as the transition from an unstable to stable atmosphere. Cloud-free conditions are determined by first removing days having significant backscatter above 5 km as determined by MPL profiles and then removing days having RH values corresponding to liquid water or ice supersaturation. Figure 1 shows several potential temperature profiles over the course of a single day (September 4, 1996). During the morning the atmosphere is stable near the surface. As the surface heats, an unstable layer developed which extends to $1200 \text{ m} \pm 200 \text{ m}$ at 1730 UTC, and $1400 \text{ m} \pm 200 \text{ m}$ at 2030 UTC.

4. Results and Discussion

In order to maximize the likelihood that the atmospheric boundary layer was well mixed, therefore meeting the assumption of estimating AOD using method I, we have restricted comparisons to measurements near midday (1730 UTC) on cloud-free days. The data pertinent to the analyses are given in Table 1, which includes boundary layer mixing heights (estimated from sonde potential temperature profiles), H_{ML} ; the mean and standard deviation of relative humidity in the lower 4 km of the atmosphere, RH_{ML} ; the RH in the sample volume of the nephelometer, RH_{neph} ; surface measurements of the aerosol scattering coefficient at 550 nm, $\sigma_{\text{sp,dry}}$; and single scattering albedo, $\omega_{\text{0,dry}}$; Ångström exponent of the light scattering coefficient (estimated using 450- and 700-nm wavelengths), $\hat{a}_{\text{neph,dry}}$; the AOD at 550 nm measured by the MFRSR, τ_{MFRSR} , and Ångström exponent (estimated using AOD values adjusted to 450- and 700-nm wavelengths) over the entire column, \hat{a}_{MFRSR} . Missing data in Table 1 represent periods when measurements were not being made or data were invalid.

4.1. Relationship Between Aerosol Extinction Coefficient at the Surface and Aerosol Optical Depth

The relationship between apparent aerosol optical depths inferred from MFRSR measurements (logarithmically interpolated to 550 nm from measurements at 499 and 608 nm), τ_{MFRSR} , versus the aerosol extinction coefficient measured at a dry RH, $\sigma_{\text{ep,dry}}$, is shown in Figure 2. The correlation of the data is weak (linear regression $r^2 = 0.55$), with a slope of 2982 m (with a 95% confidence intervals of $\pm 593 \text{ m}$), which is a rough indicator of the aerosol mixing height for the times over which the data was collected. The slopes of the linear regressions at wavelengths of 450 and 700 nm are not statistically different (at a 95% confidence interval) from the 550 nm value. The low r^2 value could be due to several possible reasons including day-to-day variability in the mixing heights at the SGP ARM site, lack of mixing of surface air with air in and/or above the boundary layer (i.e., aerosol layers exist aloft that are responsible for a significant fraction of aerosol extinction), and/or differences in aerosol physical properties (size distribution) and chemical composition with height. It is also possible that the discrepancy arises from the inability of the aerosol sampling system to transport coarse mode aerosols to the aerosol instrumentation. Although, Sheridan *et al.* [1998] report a mean ratio of submicron (diameter $< 1.0 \mu\text{m}$) to total (diameter $< 10.0 \mu\text{m}$) light scattering coefficient of 0.85 (standard deviation = 0.08), suggesting that coarse mode aerosol does not, in general, significantly influence the light scattering budget at the SGP site. The lack of a strong relationship between the extinction coefficient measured at the surface and the AOD is not surprising because of the dependence of AOD on the vertical distribution and properties of aerosols.

Figure 3 compares measured values of τ_{MFRSR} with AOD's estimated by equation (4) (τ_1) using surface measurements made at a dry reference relative humidity (i.e., $F_{\text{sp}}(\text{RH}) = F_{\text{sp}}(\text{RH}) = 1$). There is a somewhat stronger relation between τ_1 and τ_{MFRSR} (linear regression $r^2 = 0.78$) than for that between $\sigma_{\text{ep,dry}}$ and τ_{MFRSR} . This increase in correlation is attributed to the fact that τ_1 accounts for day-to-day variability in mixing heights. Estimated AOD's are systematically lower than τ_{MFRSR} . This is attributed in part to the fact that the RH values within the nephelometer are in general less than in the atmospheric boundary layer (Table 1). Therefore it is necessary to account for hygroscopic growth when

Table 1. Midday Data for Cloud-Free Days at the SGP ARM Site

Date	H_{ML} , m	RH_{ML}	RH_{neph}	$\sigma_{sp,dry}$, Mm^{-1}	$\omega_{o,dry}$	$\hat{a}_{neph,dry}$	τ_{MFRSR}	\hat{a}_{MFRSR}	τ_I (Equation 4)	τ_{II} (Equation 5)
April 10, 1996	1200	45 (10)	19	53	0.93	2.2	0.18	1.6	0.069	
June 28, 1996	1600	49 (18)	32	40	0.94	2.0	0.19	1.2	0.068	
June 29, 1996			33	50	0.97	1.9	0.26	1.4		0.16
July 3, 1996	1500	42 (13)	25	70	0.94	1.9	0.17	1.5	0.112	0.18
July 5, 1996	1600	37 (3)					0.17	1.2		
Aug. 22, 1996	1200	61 (5)	33	76	0.95	2.0	0.29	1.4	0.096	0.20
Aug. 23, 1996	1000	66 (7)	30	56	0.94	2.0	0.23	1.3	0.059	0.16
Sept. 2, 1996	1200	58 (15)	28	119	0.98	1.7	0.43	1.2	0.146	
Sept. 4, 1996	1000	57 (11)	31	74	0.95	1.7	0.25	1.4	0.078	0.15
Sept. 9, 1996	800	49 (10)	38	21	0.94	1.7	0.09	0.8	0.018	0.07
Oct. 14, 1996	1000	35 (19)	22	29	0.88	2.2	0.10	0.5	0.032	0.10
Oct. 30, 1996	800	45 (12)	9	8.5	0.89	1.8	0.04	0.4	0.008	
Nov. 2, 1996			5	5.9	0.87	1.4	0.05	0.2		
Nov. 5, 1996	1200	29 (16)	17	19	0.85	1.9	0.05	-0.04	0.027	
Dec. 12, 1996	400	39 (12)	10	52	0.95	1.5	0.08	0.6	0.022	
Dec. 13, 1996	600	27 (18)	13	97	0.92	1.7	0.12	2.0	0.063	
Jan. 16, 1997	800	27 (19)	5	12	0.93	1.0	0.06	0.4	0.010	
Jan. 17, 1997	600	31 (22)	4	13	0.96	1.2	0.07	1.2	0.008	
Jan. 20, 1997	400	26 (13)	8	28	0.91	1.8	0.04	0.6	0.012	
Jan. 22, 1997	500	30 (16)	14	12	0.92	2.0	0.15	0.2	0.007	
March 10, 1997	600	16 (12)	16	14	0.96	1.6	0.08	1.4	0.009	

RH_{ML} measurements are the average in the lower 4 km of the atmosphere, the uncertainty in H_{ML} is $\sim \pm 200$ m. The

\hat{a} values are estimated using measurements at 700 and 450 nm, all other values are at 550 nm; τ_I is estimated assuming $F_{sp}(RH)$ and $F_{ep}(RH) = 1.0$; and τ_{II} is estimated with $F_{sp}(RH)$ and $F_{ep}(RH) = 1.0$, and $\sigma_{ep}(sfc) = \sigma_{sp,dry} / \omega$.

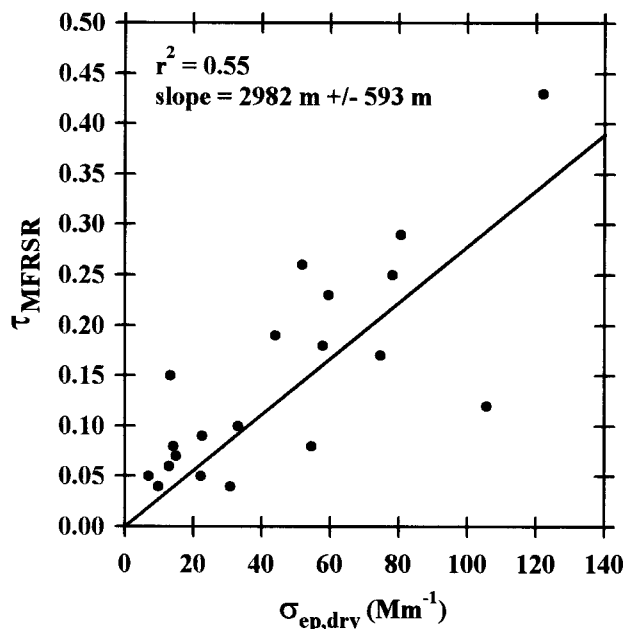


Figure 2. Aerosol Optical Depth at 550 nm estimated from MFRSR measurements, τ_{MFRSR} , versus the aerosol extinction coefficient, σ_{ep} (estimated as the sum of σ_{ap} and σ_{sp}) measured at a dry reference RH ($\sim 20\%$)

using nephelometer measurements in the estimation of atmospheric properties. Because such information is not available for the time period of the present measurements it is necessary to rely on measurements from other studies. *Rood et al.* [1987] measured $F_{sp}(RH)$ relative to a reference RH $< 35\%$ over several days in Los Angeles. The nephelometer measurements at the SGP site are made at a reference RH $< 35\%$, similar to the reference RH used by *Rood et al.* [1987]. *Rood et al.* [1987] report $F_{sp}(RH)$ values ranging from roughly 1.0 to 1.3 at an ambient RH of 30% and 1.3 to 1.7 at an ambient RH of 60%, and point out that $F_{sp}(RH)$ depends on the thermodynamic state of the aerosol (i.e. dry, subsaturated, or metastable) as well as on additional factors including the aerosol dry size distribution and chemical composition [*McInnes et al.*, 1998; *Hegg et al.*, 1993] both of which likely vary between locations. Several previous studies [*Covert et al.*, 1980; *Waggoner et al.*, 1983; *Charlson et al.*, 1984; *Dougle et al.*, 1998; *McInnes et al.*, 1998] report values of $F_{sp}(RH=60\%)$ for continental aerosols that fall within the range of values reported by *Rood et al.* [1987]. In addition, preliminary data from continuous measurements made by a dual-nephelometer humidograph system during January and February of 1999 at the SGP site show that $F_{sp}(RH=60\%)$ at 550 nm ranges from 1.1 to 1.5 (P. Sheridan, personal communication, 1998). Therefore, for the atmospheric RH values reported in Table 1 an $F_{sp}(RH)$ of 1.7 likely represents an upper limit. Figure 3 also shows lines corresponding to $\tau_{MFRSR} / \tau_I = 1.0$, and $\tau_{MFRSR} / \tau_I = 1.7$. On the basis of previous measurements the envelope of the two curves should encompass the data points if hygroscopic growth is the sole reason for the lack of agreement between τ_{MFRSR} and τ_I . Even with an assumed upper limit $F_{ep}(RH)$ value of 1.7 (assuming equivalent values for both $F_{sp}(RH)$ and $F_{ap}(RH)$), τ_I values are still systematically lower than τ_{MFRSR} by $\sim 50\%$ (standard deviation of 28%). Assuming that τ_{MFRSR} is overestimated by 0.02 due to absorption by an unknown

atmospheric species [*Halhore et al.*, 1997] results in τ_I values that are lower than τ_{MFRSR} by $\sim 40\%$, thus insignificantly contributing to the discrepancy between optical depths. These results bring into question the assumption of constant aerosol extinction with height within the mixed layer, and zero extinction above the mixed layer, that is implicit in the evaluation of τ_I by equation (4).

4.2. Estimating AOD With Surface Extinction Coefficient Measurements and Micropulse Lidar Profiles of Aerosol Backscatter

To examine the vertical distribution of aerosol we show in Figure 4 the attenuation-and range-corrected vertical profiles of aerosol 180° backscatter normalized to backscatter in the lowest MPL height range (surface to 270 m), $\beta_\pi/\beta_\pi(sfc)$. Also shown are the cumulative aerosol backscatter with height, normalized to unity, and the mixing heights as determined from radiosonde temperature profiles, H_{ML} . The measurements are for cloud-free days at 1730 UTC (~ 1130 local standard time), when, as noted above, conditions are likely to favor a well mixed boundary layer.

As is evident in Figure 4, there is considerable variation of aerosol backscatter within the mixed layer as well as substantial contribution of aerosol backscattering from altitudes above the boundary layer (i.e., above H_{ML}). The fraction of aerosol backscatter within the boundary layer, F_H , as determined by the intersections of the H_{ML} and normalized cumulative backscatter curves and estimated from equation (6), ranges from 19% to 72% (mean = 44%, standard deviation = 16%). The substantial contributions of aerosol above the boundary layer, even under the conditions of vigorous mixing, suggests that it is insufficient to omit the contribution of aerosol from above the mixed layer to AOD, at least under the conditions of the measurements reported here. That is, aerosol optical depth must explicitly employ the vertical integration of aerosol extinction (method II, equation (5)),

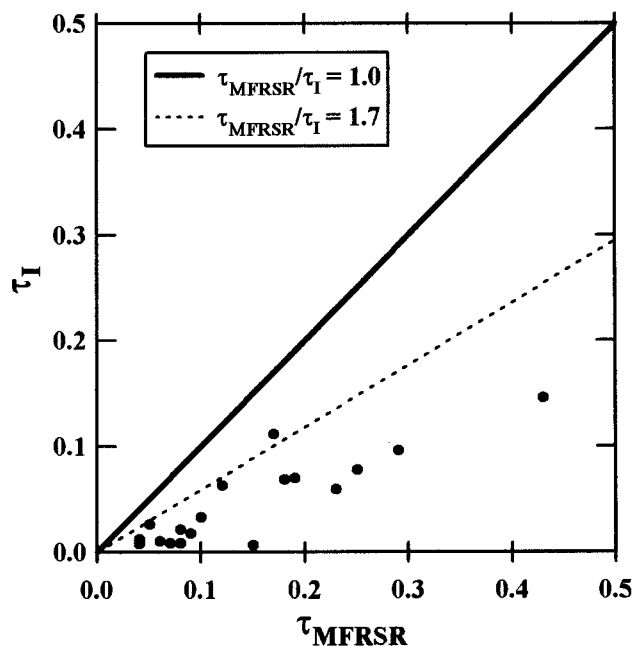


Figure 3. Aerosol Optical Depth at 550 nm estimated from extinction coefficient, σ_{ep} , measured at the surface at a dry reference RH ($\sim 20\%$), τ_I , versus τ_{MFRSR}

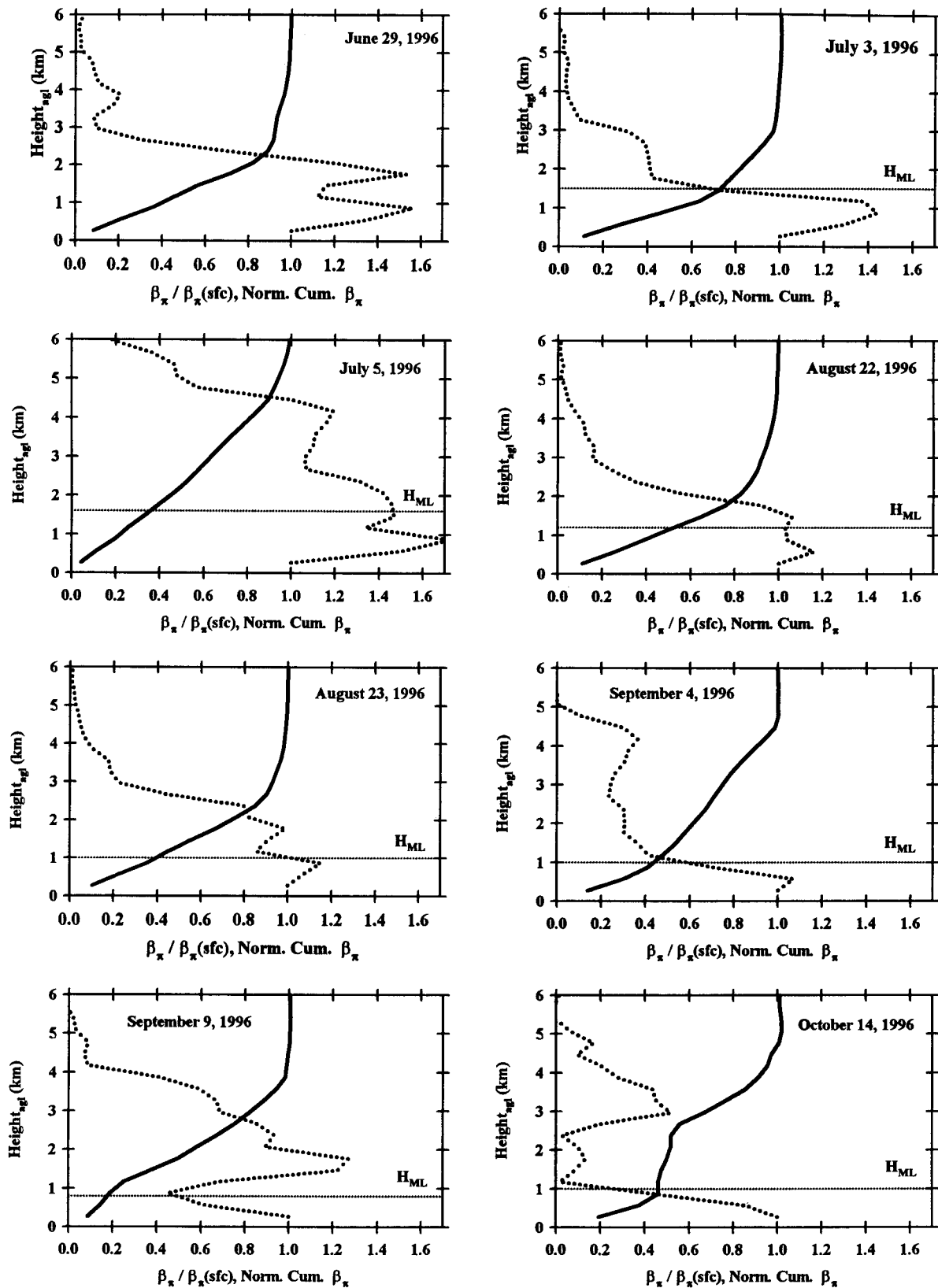


Figure 4. Attenuation- and range-corrected MPL 180° backscatter at 523 nm normalized to the backscatter in the lowest MPL range ($\beta_\pi / \beta_\pi(\text{sfc})$) (dashed line) and normalized cumulative MPL backscatter with height (solid line)

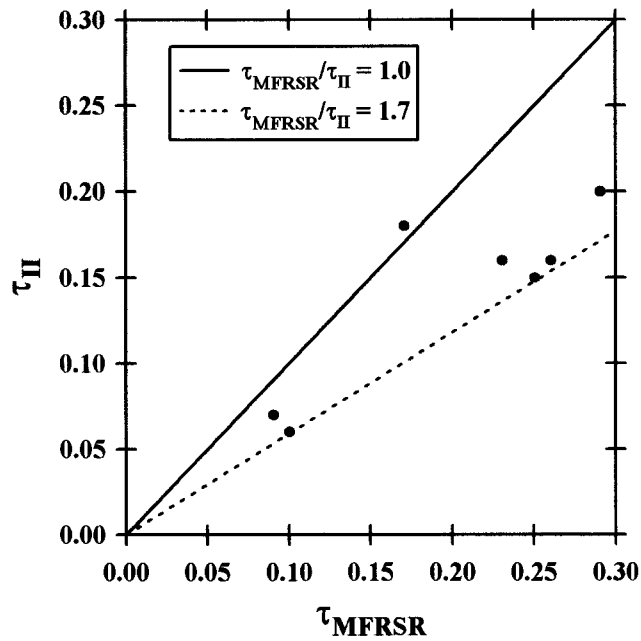


Figure 5. Aerosol optical depth at 550 nm estimated from extinction measurements at the surface scaled with MPL backscatter profiles, τ_{II} , versus the AOD measured by the MFRSR, τ_{MFRSR}

rather than assuming a uniform profile of extinction with height within the mixed layer (method I, equation (4)).

AOD's estimated from equation (5) (τ_{II}) using surface-based scattering and absorption coefficient measurements made at a dry RH ($\sim 20\%$) and MPL backscatter profiles for which both MPL and nephelometer measurements are available are shown in Figure 5 for several cloud-free days at 1730 UTC. Also shown are lines for $\tau_{MFRSR} / \tau_{II} = 1.0$ and $\tau_{MFRSR} / \tau_{II} = 1.7$; as noted above these represent the envelope of values ranging from no hygroscopic growth in the atmosphere to an upper limit hygroscopic growth factor of 1.7, as previously discussed. The ratios of τ_{MFRSR} / τ_{II} range from 0.95 to 1.6 (mean of 1.27, standard deviation of 0.22). The values of τ_{II} are thus within the range of values expected when hygroscopic growth of aerosol under atmospheric conditions is taken into account, suggesting that there is no systematic discrepancy between τ_{MFRSR} and τ_{II} when hygroscopic growth is considered. It is also important to point out that there is additional uncertainty in τ_{II} due to the assumption of a constant extinction/backscatter ratio, S_a , used in the MPL retrievals of $\beta_{\pi}(z)$. Ferrare *et al.* [1998a, b] present profiles of the aerosol extinction/backscatter ratio, S_a , determined from scanning raman lidar (SRL) measurements for several evenings during April 1994. Ferrare *et al.* [1998a, b] show that the majority of the aerosol backscatter during the night is below 2 km and that within this region S_a varies with height. Unfortunately, there is a significant ($\sim \pm 30\%$) amount of uncertainty in S_a profiles making it difficult to judge if changes in S_a with height represent actual atmospheric variability or measurement uncertainty. A 30% uncertainty in the S_a used in MPL retrievals of $\beta_{\pi}(z)$ results in an uncertainty of $\sim 10\%$ in the τ_{II} estimates shown in Figure 5. Although, if S_a is doubled values of τ_{II} increase on average by 40%, which would explain the entire discrepancy between τ_{II} and τ_{MFRSR} . It is difficult to directly relate SRL and MPL measurements since they are at different

wavelengths during different time periods. Nonetheless, the work of Ferrare *et al.* [1998a, b] clearly show the importance of directly measuring the vertical profile of S_a at the wavelength of interest in order to increase the accuracy of retrievals of aerosol backscatter profiles from lidar measurements. The overall uncertainty in estimating τ_{II} is greater than the 0.02 suggested overestimation of τ_{MFRSR} due to the atmospheric absorptance by an unknown species discussed by Halthore *et al.* [1998]. Therefore we cannot use our study to reach any conclusions as to the existence of an additional absorptance by an unknown species during clear-sky conditions.

Information on the differences in aerosol size distributions between the nephelometer and the atmosphere may be obtained by comparing the Ångström exponents for the light scattering coefficient of the dry aerosol as measured by the nephelometer, $\hat{a}_{neph,dry}$, versus that for the extinction of the atmospheric aerosol column as measured by the MFRSR, \hat{a}_{MFRSR} . Higher values of the Ångström exponent generally represent smaller particle sizes. As shown in Figure 6, \hat{a}_{MFRSR} is considerably less than $\hat{a}_{neph,dry}$ (mean value of 30% lower with a standard deviation of 23%). The uncertainty associated with \hat{a}_{MFRSR} , as shown by the error bars in Figure 6, is due to the 0.02 uncertainty in the estimation of τ_{MFRSR} (note for comparisons of \hat{a}_{MFRSR} and $\hat{a}_{neph,dry}$ we do not include \hat{a}_{MFRSR} values with uncertainties greater than the absolute value of \hat{a}_{MFRSR}). The theoretical relationship between Ångström exponent, \hat{a} , and particle size is examined in Figure 7. The Ångström exponent is estimated (using wavelengths of 700 and 450 nm) for several lognormal size distributions of specified mass median diameter (MMD) and geometric standard deviation (GSD), for spherical aerosols of refractive index 1.53 using Mie scattering theory calculations as described by Bergin *et al.* [1997]. For unimodal lognormal distributions, \hat{a} is rather sensitive to MMD and relatively insensitive to GSD. The mean values of $\hat{a}_{neph,dry}$ and \hat{a}_{MFRSR} as given in Table 1 are 1.7, and 1.3, respectively.

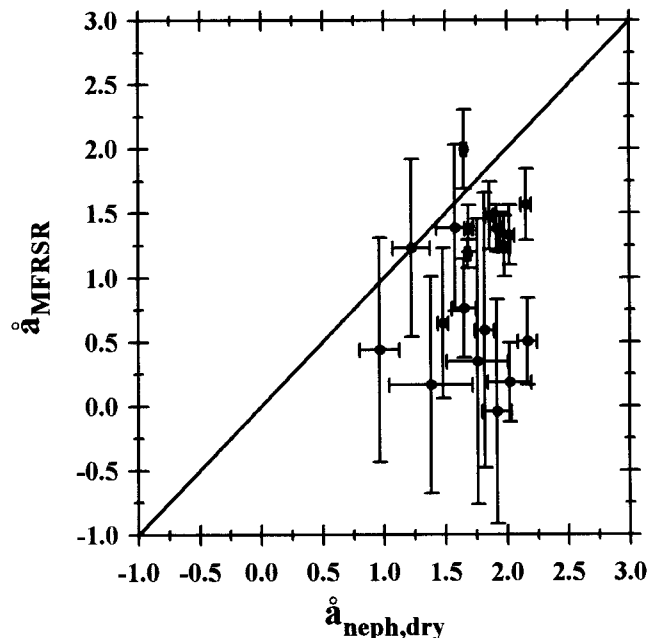


Figure 6. Nephelometer Ångström exponent, $\hat{a}_{neph,dry}$, versus MFRSR Ångström exponent, \hat{a}_{MFRSR} (estimated using 450 nm and 700 nm wavelengths)

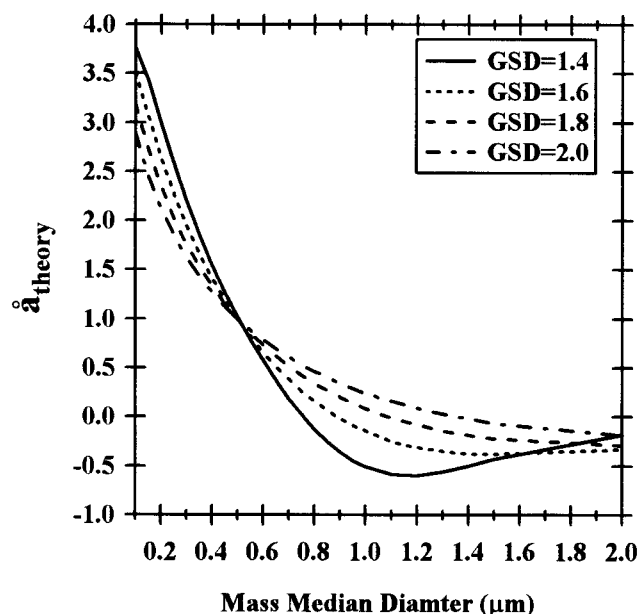


Figure 7. Theoretical estimation of Ångström exponent (estimated using 450 nm and 700 nm wavelengths), \hat{a}_{theory} , for lognormal size distributions of specified mass median diameter and geometric standard deviation, and refractive index of 1.53

According to Figure 7, this corresponds to an increase in MMD by a factor of 1.1 to 1.3. This range overlaps with the reported diameter growth factor range of 1.1 to 1.5 reported for polluted continental aerosol [Svenningsson *et al.*, 1992]. It is important to point out that changes in \hat{a} as a function of RH depend on the hygroscopic nature of the aerosol (i.e., chemical composition) and dry size distribution of the aerosol, which were not measured at the SGP site. Therefore the above discussion must be viewed as qualitative.

5. Summary and Conclusions

Two methods of estimating the aerosol optical depth have been examined using data obtained at the SGP ARM site for cloud-free days near the daily solar maximum (~1730 UTC, 1130 local standard time) at which time the boundary layer is likely to be well mixed. First, aerosol extinction measurements made at the surface (taken as the sum of the aerosol scattering and absorption coefficients at instrumental relative humidity of ~20%) are multiplied by the mixing height determined from temperature profiles from radiosonde measurements (τ_I). Second, micropulse lidar (MPL) attenuation-and range-corrected backscatter profiles are used to scale surface measurements of aerosol extinction with height (τ_{II}). The estimated AOD's are compared with measurements obtained by Sun photometry (τ_{MFRSR}).

Despite the fact that the aerosol extinction coefficient σ_{ep} contributes directly to AOD, only a weak correlation ($r^2 = 0.55$) is exhibited between AOD measured by MFRSR, τ_{MFRSR} , and aerosol extinction measurements made at the surface at a dry relative humidity (RH ~20%). Aerosol optical depths estimated from surface measurements of the aerosol extinction and mixing heights based on vertical temperature profiles exhibit somewhat better correlation ($r^2 = 0.78$). The improvement in correlation is attributed mainly to the fact that the latter approach takes into

account day-to-day variation in mixing height. Still that approach underestimates AOD by ~50% (standard deviation of 28%) even when hygroscopic growth is taken into account. The AOD's estimated using MPL backscatter profiles scaled to surface measurements of aerosol extinction at a dry RH (~20%) are lower than measured AOD's by ~30% but in agreement within the range of representative hygroscopic growth factors between the RH in the nephelometer and the atmosphere. The necessity of including the relative humidity growth factor to account for drying of the aerosols in the sampling line and nephelometer is supported by the Ångström exponents which are ~30% lower for extinction in the total column as measured by MFRSR, than those characterizing light scattering measured at the surface measured by a nephelometer. This provides strong evidence that aerosol particles in the nephelometer are generally smaller than in the atmosphere, consistent with the hypothesis that the underestimation of AOD by dry scattering coefficient measurements made at the surface is linked, in part, with the drying of aerosols within the nephelometer. The underestimation of aerosol optical depth by method I is due mainly to failure of the assumption that the aerosol is present in a well mixed boundary layer without contributions to aerosol extinction from above. As shown in Figure 4, micropulse lidar (MPL) profiles of normalized attenuation and range-corrected aerosol backscatter indicate that only ~50% of the aerosol extinction is due to boundary layer aerosol. Additional sources of error include the unknown hygroscopic growth coefficient of the aerosol as well as variation in this coefficient, and in relative humidity, from day-to-day, and with height.

The results of the present comparisons suggest that surface measurements of the aerosol scattering and absorption coefficient can be used along with information of the vertical profile of aerosol light scattering (from the MPL) and assumptions about the aerosol hygroscopicity to estimate the AOD to within roughly 30% of measured values at the SGP site. In contrast, mixing heights estimated from temperature profiles do not yield accurate estimates of AOD because of significant contribution of aerosol extinction above the boundary layer to aerosol extinction at least for this location. Overall, results show that at the SGP site it is not possible to use surface measurements to estimate aerosol optical depth without additional information on the vertical profile of aerosol extinction.

Acknowledgments. MHB was supported in part by the Global Change Distinguished Postdoctoral Fellowships program sponsored by the U.S. Department of Energy (DOE), Office of Health and Environmental Research, and administered by the Oak Ridge Institute for Science and Education. Work at Brookhaven National Laboratory was supported by the Environmental Sciences Division of the U.S. DOE, as part of the Atmospheric Radiation Measurement Program and was performed under the auspices of DOE contract DE-AC02-98CHI0886.

References

- Anderson, T. L., and J. A. Ogren, Determining aerosol radiative properties using the TSI 3563 integrating nephelometer, *Aerosol Sci. Technol.*, 29, (1), 57-69, 1998.
- Bergin, M. H., J. A. Ogren, and S. E. Schwartz, Evaporation of ammonium nitrate aerosol in a heated nephelometer: Implications for field measurements, *Environ. Sci. Technol.*, 31, 2878-2883, 1997.
- Charlson, R. J., D. S. Covert, T. V. Larson, Observations of the effect of humidity on light scattering by aerosols, in *Hygroscopic Aerosols*, edited by T. H. Ruhnke and A. Deepak, pp. 35-44, A. Deepak, Hampton, Va., 1984.

- Charlson, R. J., S. E. Schwartz, J. M. Hales, R. D. Cess, J. A. Coakley, J. R. Hansen, and D. J. Hofmann, Climate forcing by anthropogenic aerosols, *Science*, **255**, 423-430, 1992.
- Clarke, A. D., J. N. Porter, F. P. J. Valero, P. Pilewskie, Vertical profiles, aerosol microphysics, and optical closure during the Atlantic Stratocumulus Transition Experiment: Measured and modeled column optical properties, *J. Geophys. Res.*, **101**, 4443-4453, 1996.
- Covert, D. S., A. P. Waggoner, R. E. Weiss, N. C. Ahlquist, R. J. Charlson, Atmospheric aerosols, humidity and visibility, in *The Character and Origins of Smog Aerosols*, edited G. M. Hidy, Academic, 559-581, San Diego, Calif., 1980.
- Dougle, P. G., J. P. Veffkind, H. M. ten Brink, Crystallisation of mixtures of ammonium nitrate, ammonium sulphate and soot, *J. Aerosol Sci.*, **29**, (3), 375-386, 1998.
- Ferrare, R. A., S. H. Melfi, D. N. Whiteman, K. D. Evans, R. Leifer, Raman lidar measurements of aerosol extinction and backscattering, I. Methods and comparisons, *J. Geophys. Res.*, **103**, 19663-19672, 1998a.
- Ferrare, R. A., S. H. Melfi, D. N. Whiteman, K. D. Evans, M. Poellot, Y. J. Kaufman, Raman lidar measurements of aerosol extinction and backscattering, 2. Derivation of aerosol real refractive, single scattering albedo, and humidification factor using Raman lidar and aircraft size distribution measurements, *J. Geophys. Res.*, **103**, 19673-19689, 1998b.
- Halthore, R. N., S. E. Schwartz, J. J. Michalsky, G. P. Anderson, R. A. Ferrare, B. N. Holben, H. M. ten Brink, Comparison of model estimated and measured direct-normal solar irradiance, *J. Geophys. Res.*, **102**, 29, 991-30, 002, 1997.
- Halthore, R. N., S. Nemesure, S. E. Schwartz, D. G. Imre, A. Berk, E. G. Dutton, M. H. Bergin, Models overestimate diffuse and clear-sky surface irradiance: A case for excess atmospheric absorption, *Geophys. Res. Lett.*, **25**, 3591-3594, 1998.
- Harrison, L., J. Michalsky, J. Berndt, automatic multifilter rotating shadow-band radiometer: An instrument for optical depth and radiation measurements, *Appl. Opt.*, **33**, 5118-5125, 1994.
- Haywood, J. M., and K. P. Shine, The effect of anthropogenic sulfate and soot aerosol on the clear sky planetary radiation budget, *Geophys. Res. Lett.*, **22**, 603-606, 1995.
- Hegg, D., T. Larson, and P.-F. Yuen, A theoretical study of the effect of relative humidity on light scattering by tropospheric aerosols, *J. Geophys. Res.*, **98**, 18435-18439, 1993.
- Hegg, D. A., J. Livingston, P. V. Hobbs, T. Novakov, and P. Russell, Chemical apportionment of aerosol column optical depth off the mid-Atlantic coast of the United States, *J. Geophys. Res.*, **102**, 25293-25303, 1997.
- Hoppel, W. A., J. W. Fitzgerald, G. M. Frick, R. E. Larson, E. J. Mack, Aerosol size distributions and optical properties found in the marine boundary layer over the Atlantic Ocean, *J. Geophys. Res.*, **95**, 3659-3686, 1990.
- Intergovernmental Panel on Climate Change (IPCC), Radiative forcing of climate change in *Climate Change 1994*, edited by J. T. Houghton, L. G. Meira Filho, J. Bruce, H. Lee, B. A. Callander, E. Haites, N. Harris, and K. Maskel, pp. 117, Cambridge Univ. press, New York, 1995.
- Kato, S., T. P. Ackerman, E. E. Clothiaux, J. H. Mather, G. G. Mace, M. L. Wesely, F. Murcray, and J. Michalsky, Uncertainties in modeled and measured clear-sky surface shortwave irradiances, *J. Geophys. Res.*, **102**, 25881-25898, 1997.
- Kiehl, J. T., and B. P. Briegleb, Comparison of the observed and calculated clear sky greenhouse effect: Implications for climate studies, *J. Geophys. Res.*, **97**, 10037-10049, 1992.
- Koloutsou-Vakakis, S., M. J. Rood, A. Nenes, and C. Pilinis, Modeling of aerosol properties related to direct climate forcing, *J. Geophys. Res.*, **103**, 17009-17032, 1998.
- McInnes, L. M., M. H. Bergin, J. A. Ogren, S. E. Schwartz, Apportionment of light scattering and hygroscopic growth to aerosol composition, *Geophys. Res. Lett.*, **25**, 513-516, 1998.
- Michalsky, J., J. C. Liljgren, and L. C. Harrison, A comparison of Sun photometer derivations of total column water vapor and ozone to standard measures of same at the Southern Great Plains Atmospheric Radiation Measurement site, *J. Geophys. Res.*, **100**, 25995-26003, 1995.
- Ogren, J. A., and P. A. Sheridan, Vertical and horizontal variability of aerosol single scattering albedo and hemispheric backscatter fraction over the United States, *Proceedings of the Conference on Nucleation and Atmospheric Aerosols*, pp.780-783, Univ. of Helsinki, Helsinki, Finland, 1996.
- Ogren, J. A., S. Anthony, J. Barnes, M. H. Bergin, W. Huang, L. M. McInnes, C. Myers, P. Sheridan, S. Thaxton, and J. Wendell, Aerosols and radiation, *Summ. Report 1994-1995*, NOAA Climate Monit. And Diag Lab., 1996.
- Penner, J. E., R. J. Charlson, J. M. Hales, N. Laulainen, R. Leifer, T. Novakov, J. A. Ogren, L. F. Radke, S. E. Schwartz, and L. Travis, Quantifying and minimizing uncertainty of climate forcing by anthropogenic aerosols, *Bull. Am. Meteorol. Soc.*, **75**, 375-400, 1994.
- Quinn, P. K., T. L. Anderson, T. S. Bates, R. Dlugi, J. Heintzenberg, W. von Hoyningen-Huene, M. Kulmala, P. B. Russell, E. Swietlicki, Closure in tropospheric aerosol-climate research: A review and future needs for addressing aerosol direct shortwave radiative forcing, *Beitr. Phys. Atmo.*, **69** (4), 547-577, 1996.
- Remer, L. A., S. Gasso, D. A. Hegg, Y. J. Kaufman, and B. N. Holben, Urban/industrial aerosol: Ground-based sun/sky radiometer and airborne in situ measurements, *J. Geophys. Res.*, **102**, 16849-16859, 1997.
- Rood, M. J., D. S. Covert, and T. V. Larson, Hygroscopic properties of atmospheric aerosol in Riverside, California, *Tellus, Ser. B.*, **39**, 383-397, 1987.
- Schwartz, S. E., The whitehouse effect-shortwave radiative forcing of climate by anthropogenic aerosols: An overview, *J. Aerosol Sci.*, **3**, 359-382, 1996.
- Schwartz, S. E., and M. O. Andreae, Uncertainty in climate change caused by aerosols, *Science*, **272**, 1121-1122, 1996.
- Sheridan, P. J., J. Barnes, M. Bergin, M. Doorenbosch, W. Huang, A. Jefferson, J. Ogren, J. Wendell, Aerosols and Radiation, *NOAA/Clim. Monit. and Diag. Lab., Summ. Rep. 1996-1997*, Boulder, Colo., 1998.
- Spinhirne, J. D., Micropulse lidar, *IEEE Trans Geosci. Remote. Sens.*, **31**, 48-55, 1993.
- Spinhirne, J. D., J. A. Reagan, B. M. Herman, Vertical distribution of aerosol extinction cross section and inference of aerosol imaginary index in the troposphere by lidar technique, *J. Appl. Meteorol.*, **19**, 426-438, 1980.
- Svenningsson, I. B., H.-C. Hansson, A. Wiedensohler, J. A. Ogren, K. J. Noone, and A. Hallberg, Hygroscopic growth of aerosol particles in the Po Valley, *Tellus, Ser. B* **44**, 556-569, 1992.
- Tang, I. N., Deliquescence properties and particle size change of hygroscopic aerosols, in *Generation of Aerosols and Facilities for Exposure Experiments*, edited K. Willeke, Ann Arbor Science, Ann Arbor, Mich., 1980.
- Veefkind, J. P., and J. C. H. van der Hage, H.M. ten Brink, Nephelometer derived and directly measured AOD of the atmospheric boundary layer, *Atmos. Res.*, **41**, 217-228, 1996.
- Waggoner, A. P., R. E. Weiss, and T. V. Larson, In-situ rapid response measurement of H₂SO₄/(NH₄)₂SO₄ aerosols in urban Houston: A comparison with rural Virginia, *Atmos. Environ.*, **17**, 1723-1731, 1983.

M. H. Bergin, School of Civil and Environmental Engineering and, School of Earth and Atmospheric Sciences, Georgia Institute of Technology, Atlanta, GA 30332-0512. (mike.bergin@ce.gatech.edu).

R. N. Halthore and S. E. Schwartz, Brookhaven National Laboratory, Environmental Chemistry Division, Upton, NY 11973-5000.

D. L. Hlavka, Science Systems and Applications Division, NASA Goddard Space Flight Center, Greenbelt, MD 20771.

J. A. Ogren, Climate Monitoring and Diagnostics Laboratory, NOAA, Boulder, CO 80303.

(Received October 14, 1998; revised May 27, 1999; accepted June 3, 1999.)